Ball milled SnO$_2$: a modified vapor source for growing nanostructures

Tao Tao [a,b], Alexey M. Glushenkov [a,*], Huiping Hu [b], Qiyuan Chen [b], Ying Chen [a]

[a] ARC Centre of Excellence for Functional Nanomaterials, Institute for Technology Research and Innovation, Deakin University, Waurn Ponds, Victoria 3217, Australia
[b] College of Chemistry and Chemical Engineering, Central South University, Changsha 410083, China

ARTICLE INFO

ABSTRACT

The evaporation behaviour of a ball milled SnO$_2$ powder has been investigated. It is observed that the milled powder starts to evaporate at the temperatures above 950 °C while the unmilled SnO$_2$ powder does not generate any vapor at this temperature. The effect is likely to be related to structural changes in the milled material and, particularly, a certain degree of reduction of the SnO$_2$ powder in the course of milling. The milled powder can be used as a vapor source for producing various types of nanostructures of SnO$_2$.

© 2010 Elsevier B.V. All rights reserved.

1. Introduction

One-dimensional (1D) nanostructures of semiconducting oxides have attracted great interest and much progress has been achieved due to their many interesting physical properties and great potential applications in ultra-sensitive chemical and biological nanosensors, cross-wire junction based devices, nanogenerators, and nano-piezotronics [1]. A rich family of 1D nanostructures of semiconducting oxides has been already described in the literature including nanowires, nanoribbons, nanotubes, nanorods, and so forth [2–6]. Nanomaterials of tin oxide are particularly important functional materials with high surface to volume ratio, chemical stability, remarkable resistivity variation in a gaseous environment, and high exciton binding energy of 130 MeV [7–9].

Thermal evaporation technique is possibly the most popular method for preparation of 1D nanostructures of semiconducting oxides. Although it is currently widely used, the method of thermal evaporation has drawbacks such as low quantities of products and often high temperature required for evaporation [2]. One possible way to overcome those is to design novel vapor sources that can generate more vapor or evaporate at a lower temperature.

In this paper, we demonstrate that milled SnO$_2$ powder can evaporate at above 950 °C while unmilled SnO$_2$ does not generate any vapor at such temperatures. Various kinds of nanostructures such as SnO$_2$ nanoribbons, nanobranches, nanocrystals and SnO nanodiskettes can be synthesized by using the ball milled powder as an evaporation source.

2. Experimental

Three–four grams of SnO$_2$ powder (Sigma–Aldrich, 99.9% purity, Sublimation point: 1800–1900 °C, Melting point: 1630 °C) were milled for 100 h at room temperature in a magneto-ball mill with four hardened steel balls (diameter of 25.4 mm) under Ar atmosphere of 100 kPa. The magnet was located at the bottom of the mill at a 45° position in relation to the vertical direction and the rotation speed was 160 rpm.

To compare the evaporation patterns of two vapor sources, a series of experiments was conducted and the weight losses of the milled and unmilled SnO$_2$ samples after annealing for various periods of time (between 20 min and 2 h) inside of the tube furnace in Ar flow (100 ml/min) at 1100 °C were measured. A boat loaded with a SnO$_2$ powder (in the original powder form) was placed in the center of a horizontal tube furnace in each experiment, and the weight losses after annealing for various periods of time were recorded. In addition, a thermogravimetric (TGA) experiment has been conducted using a Shimadzu TGA-60 instrument in N$_2$ flow and at the heating rate of 20 °C/min.

In the first synthesis experiment the milled SnO$_2$ powder was heated from room temperature to 1100 °C (30 min), kept at this temperature for 120 min, and naturally cooled down to room temperature in an Ar flow (100 ml/min). After annealing, nanobranches (gray-white layer) and nanodiskettes (gray-black layer) products were collected in the low temperature region of 100–300 °C downstream 20 cm away on the inner wall of alumina tube. When the gas flow speed was reduced below 50 ml/min, nanoribbons (white cotton-like layer) were collected in the high temperature region of 800–900 °C located downstream 7.5 cm away from the location of the source.

In the second synthesis experiment the milled SnO$_2$ powder was heated at 1050 °C for 120 min in Ar gas flow (50 ml/min) and naturally cooled down to room temperature with access of air. After annealing, a large percentage of milled powder was transformed into nanocrystals in the alumina boat.

The nanostructures of SnO$_x$ produced and powder samples were characterized using X-ray diffraction (XRD) (Philips 3020, Co target, 40 kV, 30 mA, λ = 0.1789 nm).
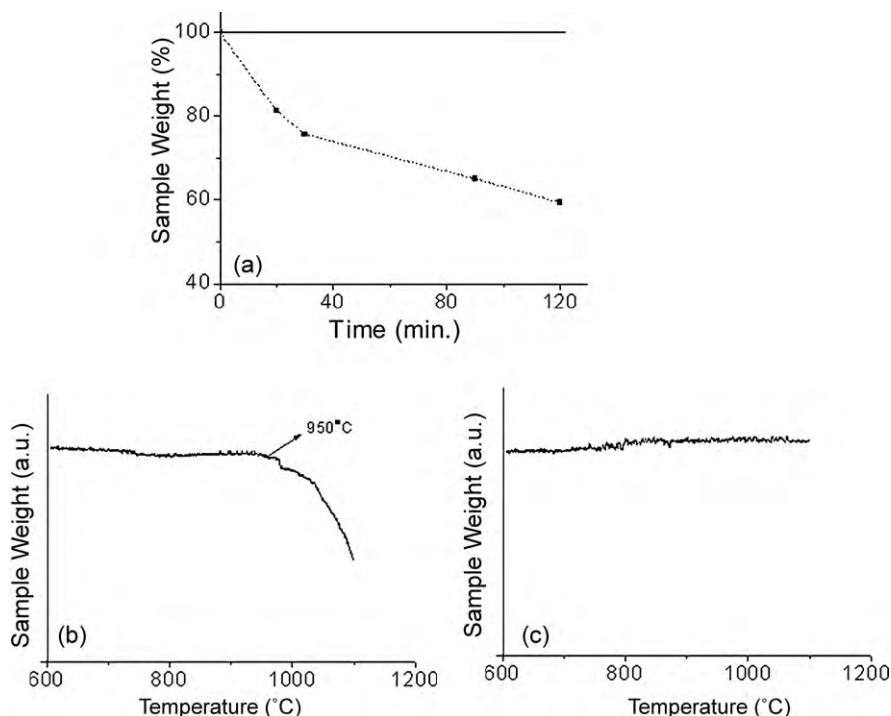
Fig. 1. (a) Weight loss as a function of annealing time: unmilled SnO_2 (solid line), SnO_2 milled for 100 h (dotted line), and TGA curves (b and c) for milled SnO_2 (b) and unmilled SnO_2 (c).

Scanning electron microscopy (FESEM, Zeiss UltraPlus) was used to characterize the morphology of the samples, and X-ray energy-dispersive spectrometry (EDS) was conducted in the SEM for determining chemical composition information.

3. Results and discussion

Fig. 1a shows the weight loss of the milled SnO_2 and unmilled SnO_2 samples after heating in the tube furnace for various periods of time in Ar gas flow (100 ml/min) at 1100 °C. After 120 min of heat treatment, the milled sample lost 40.6 wt.%. The milled powder clearly evaporates at a significant rate of at least 0.18% per minute, and a faster evaporation rate in the first 30 min could be due to a certain initial overheating of the furnace above 1100 °C or the presence of a very volatile fraction in the material. No weight loss was detected from the unmilled samples under the same condi-

tions (Fig. 1a). Hence, the curves (solid for the original sample and dotted for the milled one) in Fig. 1a clearly indicate the enhanced evaporation of SnO_2 powders induced by ball milling treatment.

Fig. 1b and c displays the TGA curves of the two samples showing weight changes during heating up to 1100 °C. Noticeable weight loss from the milled sample (Fig. 1b) can be detected when the temperature is above 950 °C, and the unmilled sample does not lose weight (Fig. 1c), which is consistent with the expected behaviour of a commercial SnO_2 powder.

The SEM image in Fig. 2a shows the typical agglomerates of the mechanically milled SnO_2 powder that consist of particles of various sizes with irregular shapes. In contrast to the XRD pattern of unmilled SnO_2 powder (Fig. 2b), the diffraction peaks of the milled SnO_2 powder are weak and broad (Fig. 3c). The broadening of the peaks happens due to the nanocrystalline nature of the ball milled
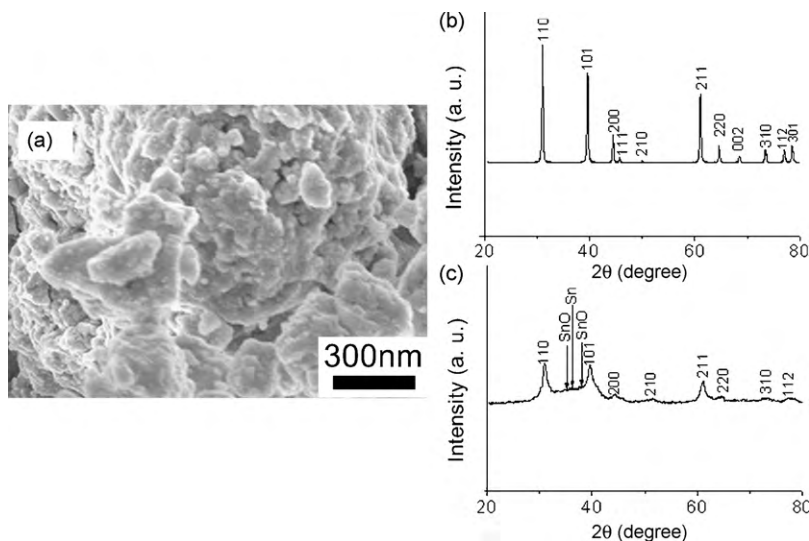
Fig. 2. SEM image (a) for milled SnO_2 and XRD patterns (b and c) for the unmilled and milled SnO_2 powders, respectively.
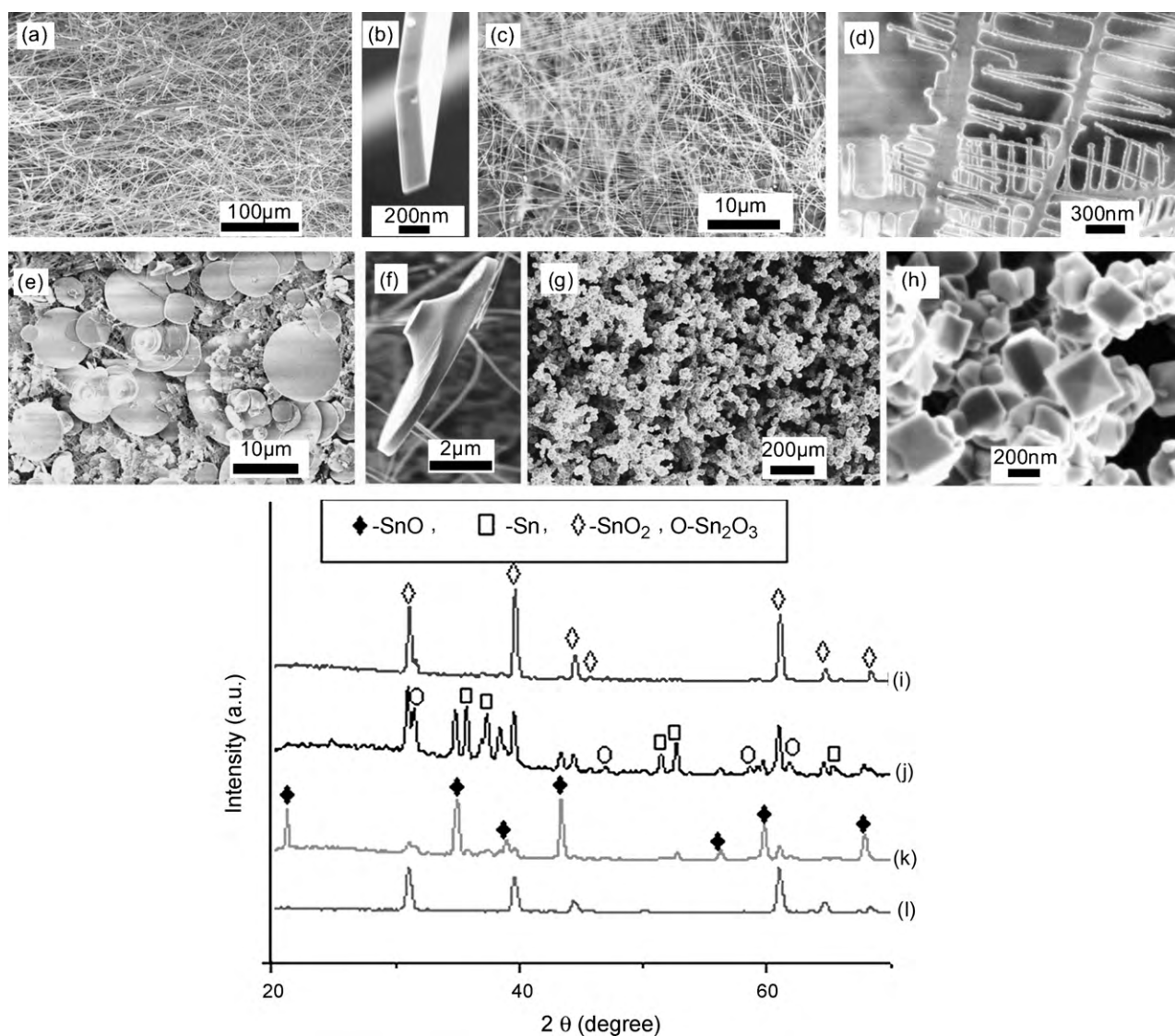
Fig. 3. Typical SEM images of the products obtained from the milled SnO$_2$ powder: (a and b) nanoribbons; (c and d) nanobranches; (e and f) nanodiskettes; (g and h)nanocrystals; and XRD patterns for nanoribbons (i); nanobranches (j); nanodiskettes (k) and nanocrystals (l).

powder. The creation of nanocrystalline structure is a typical well-known effect of ball milling [10]. The grain size calculated from the XRD data cannot be used as an estimate of particle size because the particle size may be an order of magnitude larger.

The results show that unmilled SnO$_2$ sample is very stable at 1100 °C, and its evaporation behaviour is completely different from that of the milled SnO$_2$ powder. Significant amounts of vapor are continuously produced from evaporation of the milled SnO$_2$ sample for the duration of at least two hours. A TGA experiment supports the observation and indicates 950 °C as the onset of evaporation. A possible reason for the observed increased evaporation rate could be the presence of Fe in the sample coming from milling balls and containers. Theoretically, iron impurities could reduce SnO$_2$ to SnO and Sn, which can evaporate at low temperatures. However, only about 3.9 wt.% Fe was found in the sample which is not large enough to reduce SnO$_2$ to a significant extent (up to 40% in our experiment). Obviously, the enhanced evaporation of the milled SnO$_2$ powder has an origin different from iron contaminations.

Begin-Colin et al. have previously studied phase transformations induced by mechanical milling in SnO$_2$ [11]. Using ^{119}Sn Mössbauer spectroscopy, these authors proved that SnO$_2$ was getting reduced during milling *in situ*. According to their data, the change in the

oxygen content in SnO$_2$ happened via the mechanism involving the reduction at the interface between the balls and the powder (on the surface of balls). The coating of the balls has been analysed and concluded to have a composition of SnO$_{1.7}$. As a result of the process described by Begin-Colin et al., the powder could get reduced while it could avoid being contaminated by iron impurities significantly. Although we have used a different milling apparatus and milling parameters, it is highly likely that similar structural changes may happen in our case as well.

It is possible that SnO$_2$ can be reduced in our experiment even further than in the experiments of Begin-Colin et al. [11]. The XRD pattern of the milled sample (Fig. 2c) reveals a broad feature between the (1 1 0) and (1 0 1) peaks of SnO$_2$. The strong peaks in XRD patterns of Sn and SnO have positions which are indicated by arrows in Fig. 2c and are located just between (1 1 0) and (1 0 1) peaks of SnO$_2$. The broad feature observed in the experimental XRD pattern may be at least partially composed by the superposition of broadened Sn and SnO peaks in this area.

The idea about milling-induced reduction is in line with experimental observations. The evaporation rate of the milled SnO$_2$ material can be particularly fast in the beginning due to the presence of certain amount of Sn and SnO. After 30 min of annealing,

the rate of evaporation of the milled material stabilizes at the level of 0.18% per min. We speculate that only slightly reduced bulk SnO_x continues to evaporate at this stage after the full amount of Sn and SnO phases left the sample. Based on the above, the efficient evaporation at a lower temperature can be correlated with the reduction of SnO_2 during ball milling.

We have demonstrated that the milled SnO_2 sample can be used to synthesize a range of important nanostructures of tin oxide at a low temperature of 1050–1100 °C. A typical morphology of SnO_2 nanoribbons with lengths of tens and hundreds of micrometers, width and thickness of about 100–500 and 10–50 nm, respectively is shown in Fig. 3a and b. Nanobranches (Fig. 3c and d) represent another morphology which we have produced by the evaporation of the ball milled SnO_2. The typical morphology of nanodiskettes whose diameter is 8–10 μm and thickness is between several tens and several hundreds of nanometers, is shown in Fig. 3e and f. The SEM images of typical SnO_2 nanocrystals with regular shapes and width of about 50–500 nm can be seen in Fig. 3g and h. XRD patterns of samples containing nanoribbons, nanobranches, nanodiskettes and nanocrystals are presented in Fig. 3i–l. The XRD spectrum of nanoribbons and nanocrystals in Fig. 3i and l shows that the phase of products corresponds to the tetragonal rutile phase of SnO_2 with lattice constants $a = 0.47358$ nm and $c = 0.31851$ nm (JCPDS No. 41-1445). No characteristic peaks of impurities, such as elemental tin or other tin oxides, are observed. The XRD spectrum of nanobranches in Fig. 3j shows measurable quantities of SnO_2, Sn, SnO, and Sn_2O_3 phases coexisting in the sample. As it can be seen from Fig. 3k, nanodiskettes mainly consist of SnO, and the diffraction peaks can be indexed as those of the tetragonal structure with lattice constants of $a = 0.3802$ and $c = 0.4836$ nm (JCPDS No. 06-0395). Small amounts of Sn, Sn_2O_3 and SnO_2 are also detected.

The likely formation mechanism of SnO_2 nanoribbons is a vapor–solid (VS) process since no metal particles have been found attached to the tips of nanoribbons [12]. The formation of tin oxide nanobranches follows a vapor–liquid–solid (VLS) process reported before [13]. The nanodiskettes are formed by a solidification (liquid–solid) process and represent a well-known morphology of SnO (see, for example, Ref. [3]). SnO_2 nanocrystals may form during the cooling stage of the experiment when significant vapor condensation inside of the combustion boat is possible.

4. Conclusions

We have shown that a milled SnO_2 powder has much better evaporation ability than a conventional (unmilled) powder. The milled SnO_2 powder evaporates at a significant rate at 1100 °C. After 120 min of heat treatment, the milled sample lost 40.56 wt.% while unmilled SnO_2 was unable to generate any vapor under the same heating conditions. A TGA experiment indicated that the evaporation of the ball milled SnO_2 started at about 950 °C. Milled SnO_2 powders can be used as efficient vapor sources to grow nanostructures of tin oxide such as SnO_2 nanoribbons, nanobranches, nanocrystals and SnO nanodiskettes by thermal evaporation.

Acknowledgments

References

[1] Z.L. Wang, J. Nanosci. Nanotechnol. 8 (2008) 27–55.
[2] Z.R. Dai, Z.W. Pan, Z.L. Wang, Adv. Funct. Mater. 13 (2003) 9–24.
[3] Z.R. Dai, Z.W. Pan, Z.L. Wang, J. Am. Chem. Soc. 124 (2002) 8673–8680.
[4] A.M. Glushenkov, V.I. Stukachev, M.F. Hassan, G.G. Kuvshinov, H.K. Liu, Y. Chen, Cryst. Growth Des. 8 (2008) 3661–3665.
[5] O. Lupan, L. Chow, G. Chai, A. Schulte, S. Park, H. Heinrich, Mater. Sci. Eng. B 157 (2009) 101–104.
[6] P. Billik, M. Čaplovičová, Powder Technol. 191 (2009) 235–239.
[7] D. Calestani, M. Zha, A. Zappettini, L. Lazzarini, G. Salviati, L. Zanotti, G. Sberveg\-lieri, Mater. Sci. Eng. C 25 (2005) 625–630.
[8] F. Li, L.Y. Chen, Z.Q. Chen, J.Q. Xu, J.M. Zhu, X.Q. Xin, Mater. Chem. Phys. 73 (2002) 335–338.
[9] J. Yang, K. Hidajat, S. Kawi, J. Mater. Chem. 19 (2009) 292–298.
[10] Y. Chen, M. Bibole, R. Le Hazif, G. Martin, Phys. Rev. B 48 (1993) 14–21.
[11] S. Begin-Colin, G.L. Caer, M. Zandona, E. Bouzy, B. Malaman, J. Alloys Compd. 227 (1995) 157–166.
[12] Z.L. Wang, Z.W. Pan, Adv. Mater. 14 (2002) 1029–1032.
[13] Z.W. Pan, Z.R. Dai, Z.L. Wang, Science 291 (2001) 1947–1949.